IJMF, Iranian Journal of Materials Forming, Vol. 3, No. 1, pp 12-26
Printed in The Islamic Republic of Iran, 2016

Numerical Investigation of Circular Plates Deformation under Air Blast Wave

B. Veisi, K. Narooei * and J. Zamani
K. N. Toosi University of Technology, Tehran, Iran

Abstract: In the current research the maximum deflection of circular plates made of the AA5010 and AA1100 alloys under blast load was investigated. Shock waves were produced by exploding a spherical charge in different distances from the center of plates. The ABAQUS software uses the conwep equation for the blast loading analysis. It was found that the results of these simulations have about 30% to 40% inaccuracy in comparison with experimental results. To improve the accuracy of simulations, the Friedlander equation was used that considers the positive phase of blast wave as exponential and the negative phase as bi-linear function. To this goal, the VDLOAD subroutine was developed. Results were shown the difference between the experimental and simulation data was decreased to 8%. Moreover, the effect of uniform and non-uniform shock waves on deformation of structure and various failures were investigated. It was observed that uniform shock waves can be attained when the minimum distance of exploding charge and plate is about 3 times of the radius of plate.

Keywords: Blast loading, Friedlander equation, Circular plate, Failure, Explosive forming.

1. Introduction

Experimental tests are the best method for investigation of blast loading effects on structures. However, experimental specimens, explosive charges, and measurement equipment (like pressure sensors) cannot be reused. Also, experimental tests are expensive and may be dangerous. On the other hand, numerical simulations which study the effects of shock loading on structures have the properties of repeatability, safety, and low costs. Behavior of structures under the blast loading has been studied by many researchers during recent years. Travis et al. [1] in 1961 and Johnson et al. [2] in 1966 investigated response of circular plates under blast loading experimentally. They used Pin-contactors and measured the time-displacement histories. Vendhan et al. [3] in 2000 studied the nonlinear dynamic behavior of rectangular plates loaded with shock waves of underwater explosion. In this research, plates made of mild steel and HSS subjected in water tank and the plastic deformation were measured under PEK-L explosive charge. In 2005, Baldwin and Nurick [4] simulated the dynamic behavior of steel sheets under blast loading. They modeled explosive charge as a layer on sheet and investigated the failure behavior of sheets. Neuberger et al. [5] in 2007 simulated the dynamic behavior of thick armored steel sheets under different TNT spherical charges. They used solid elements for meshing of sheets and material was considered as elastic-viscoplastic by Johnson-Cook model. McShane et al. [6] in 2008 investigated deformation of two-layer circular plates under shock wave. These plates were made of the copper and polyethylene layers. They studied the deformation behavior under the dynamic and quasi-static conditions. Narooei and Karimi Taheri [7] in 2009 considered the formability of aluminum and steel sheets in stretch forming process using assumed strain finite element methods. Setoodeh et al. [8] in 2009 simulated the armored steel plates under blast loading. They used the C4 and TNT charges. Neuberger et al. [9] in 2009 experimentally and numerically investigated the spring-back of circular clamped armor steel plates subjected to spherical air-

Received by the editors January 24, 2016; Revised March 11, 2016 and Accepted March 12, 2016.
*Corresponding author (knarooei@kntu.ac.ir)

blast loading. As the conwep equation was used in their simulations, they reported 30% discrepancy with respect to experimental results. In 2010, Langdon et al. [10] studied tearing of aluminum panels of the foam core and a sacrificial coating under blast loading. They assessed the effects of core density and thickness of the coating. Zamani et al. in 2011 [11] inspected the effect of strain rate on fully clamped aluminum and steel circular plates loaded with underwater blast loading. Goel et al. [12] in 2011 studied the dynamic response of stiffened plates under rectangular pulse blast loadings in ABAQUS/Explicit. Kumar et al. [13] in 2012 investigated bending of plates under blast loading experimentally and considered one of the plates flat and others had curvature with different radii. To apply shock waves on these plates, a shock tube was used. In order to record speed and deformation, a three-dimensional digital camera and sequential imaging technique were used. They mentioned the plastic deformation of plates with small curvature was minimum. Spranghers et al. [14] in 2013 studied the dynamic response of aluminum plates under the blast loading. To increase the accuracy of simulations, the LBE method was used. Longere et al. [15] in 2013 investigated the fracture behavior of a ship structure under near-field air-blast loading and simulated the structural response using the ABAQUS software and the conwep function. Tavakoli and Kiakojouri [16] in 2014 investigated the dynamic behavior of stiffened steel sheets under blast waves in ABAQUS/Explicit. Blast loading was considered as a triangular pulse. Also, effects of stiffener geometry, mesh density, damping coefficient, and strain rate were studied. They presented two optimized models for reducing deflection. Sitnikova et al. [17] in 2014 modeled the perforation failure in fiber metal laminates subjected to high impulsive blast loading in ABAQUS software. Explosion load was applied to structures as exponential and rectangular pulses. Jha and Kumar [18] in 2014 simulated the blast wave in the ANSYS/AUTODYN software and the incident pressure in air was compared with the Kinney-Graham and conwep equation results. Results of the conwep equation modeling showed 20 percent inaccuracy with respect to results of the incident pressure in air. Johnson et al. [19] in 2015 numerically studied the bioinspired nacre-like composite plates under blast loading in ABAQUS software. Micallef et al. [20] in 2016 used the ABAQUS/Explicit for numerical study of the dynamic plastic response of steel membranes subjected to localized blast loading. They considered load function as a rectangular pulse.

According to above brief discussion, using the conwep equation for modeling of the explosive forming causes inaccuracy due to nature of the model and neglecting of the negative phase. Hence, in the current research, the explosive forming of aluminum circular plates was investigated using the Friedlander equation to consider the negative phase. As the Friedlander equation does not exist in ABAQUS software, a VDLOAD subroutine was prepared. The positive phase of blast wave was considered as the exponential function and the negative phase was assumed as bi-linear function. In the next section the experimental tests that were performed in the Modern Metal Forming Laboratory of K. N. Toosi University of Technology, are presented. In the section 3 the simulation procedure is explained. To consider the damage in the explosive forming process the Johnson-Cook criterion is described. Finally, the results of simulations are compared with the experimental results.

2. Experimental Tests

In the blast loading process, chemical changes occur rapidly and cause physical disturbances and travel of resultant waves together. The schematic of shock wave was shown in Fig. 1. In fact, producing a shock wave is the first step in blast phenomenon. The speed of wave propagation is about several times of the speed of sound and this speed reduces quickly. In air blast, the pressure of a specific point from an explosive charge reaches the maximum pressure and then reduces exponentially (positive phase). The pressure decreases further and finally it comes back to the ambient pressure (negative phase).

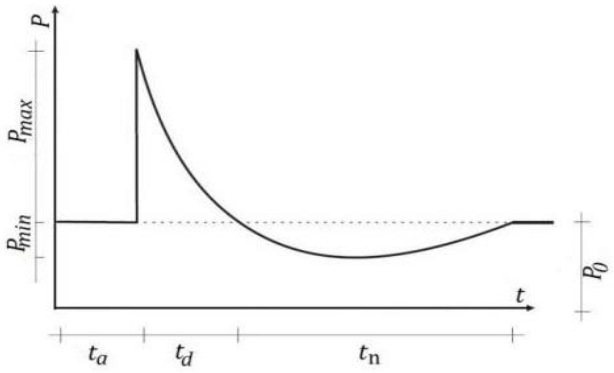

Fig. 1. Pressure-time air blast wave [21].

In order to study the deformation of fully clamped circular plates under the blast loading, tests were taken on circular specimens made of aluminum alloys with 240 mm diameter and 2-3 mm thickness. The spherical charges of C4 used for producing of blast waves. In these tests different masses of explosive charges were located on the symmetry axis of plates in different distances. Clamping of aluminum plates in the blank holder located a circular area with diameter of 170 mm under the blast waves. To study effects of non-uniform shock waves, ten tests were carried out on AA5010 such that the distance between plates and explosive charges be less than three times of the plate radius (table 1). To take into account effects of uniform shock waves, nine tests on AA1100 were designed (table 2). The deformed shape of exploded samples was measured by CMM apparatus. As it can be seen from Fig. 2a about sixty points in different radii of each sheet were selected for measurement of deformed profile with respect to reference surface on the top of the sheet and under the blank holder. The pressure of exploded mass was extracted from the standard tables of reference [22]. The blast parameters were presented in tables 1 and 2. In these tables s, r, t, w, and z represent charge distance from sheet, radius under blast loading, thickness of sheet, mass of C4, and the scaled distance respectively. In the next section the simulation method is described.

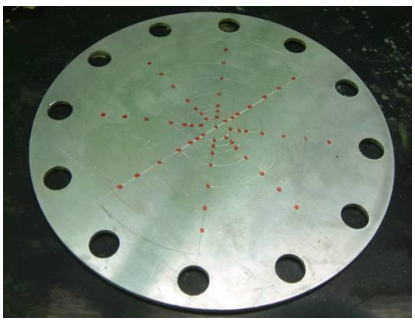

(a)

(b)

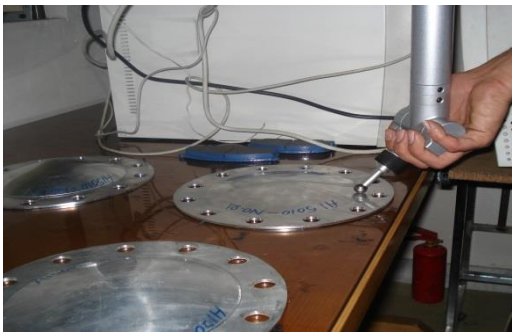

(c)

Fig. 2. Air-blast experimental set-up: (a) blank, (b) die equipment, (c) sensor device for taking data.

Table 1. Air-blast experimental parameters (AA5010).

Test no.	W (Kg)	S (m)	r (mm)	t (mm)	Z (m/kg$^{1/3}$)
1	0.03	0.2	85	3	**0.5838**
2	0.03	0.1	85	3	**0.2919**
3	0.05	0.12	85	3	**0.2955**
4	0.06	0.12	85	3	**0.2780**
5	0.07	0.12	85	3	**0.2641**
6	0.07	0.2	85	3	**0.4402**
7	0.07	0.15	85	3	**0.3301**
8	0.075	0.15	85	3	**0.3226**
9	0.09	0.15	85	3	**0.3036**
10	0.115	0.15	85	3	**0.2798**

Table 2. Air-blast experimental parameters (AA1100).

Test no.	W (Kg)	S (m)	r (mm)	t (mm)	Z (m/kg$^{1/3}$)
11	0.051	0.3	85	2	**0.7352**
12	0.088	0.3	85	2	**0.6125**
13	0.061	0.35	85	2	**0.8078**
14	0.081	0.4	85	2	**0.8396**
15	0.091	0.4	85	2	**0.8075**
16	0.097	0.4	85	2	**0.7905**
17	0.124	0.4	85	2	**0.7282**
18	0.081	0.5	85	2	**1.0495**
19	0.101	0.5	85	2	**0.9748**

3. Simulation procedure

According to dimensions of experimental specimens, the geometrical model was prepared and it can be seen in Fig. 3. In the simulations, the convectional shell model was used. In high-frequency loading such as blast phenomena, loads are applied in a very small period of time to structures. Therefore, the implicit time integration is impossible due to larger stable time increments with respect to the explicit time integration. Moreover, using the small time increments in implicit time integration caused very large computational time. As by decreasing time increments, discrepancy of the explicit and implicit time integration is decreased, researchers prefer to use the explicit time integration in explosion phenomena [15, 16, 20, and 23]. The mechanical and physical properties of specimens were given in table 3. To consider the strain rate effect, the Johnson-Cook model was used as:

$$\bar{\sigma} = \left[A + B\bar{\varepsilon}^{n}\right]\left[1 + C\ln\left(\frac{\dot{\bar{\varepsilon}}}{\dot{\varepsilon}_0}\right)\right]\left[1 + \left(\frac{T - T_r}{T_m - T_r}\right)^{m}\right] \quad (1)$$

where $\bar{\sigma}$ is the flow stress, C strain rate constant, $\dot{\bar{\varepsilon}}$ plastic strain rate, $\dot{\varepsilon}_0$ reference strain rate, T specimen temperature, T_m melting temperature, T_r room temperature, A, B, n, and m are the Johnson-Cook plasticity constants which can be seen in table 4 [24, 25].

To achieve the clamped boundary conditions under the blank holder, plates were fixed in a margin of 20 mm as illustrated in Fig. 3.

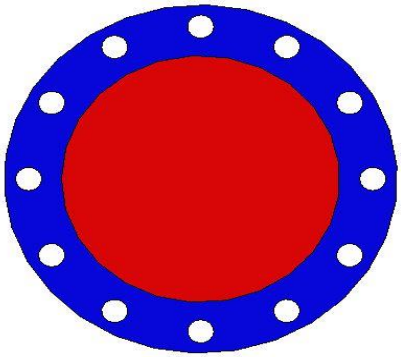

Fig. 3. Sheet geometry used in ABAQUS: center part under blast wave and margin under blank holder.

Table 3. Mechanical and physical properties of plates.

Material	Ultimate Stress (MPa)	Yield Stress (MPa)	Elasticity Modulus (GPa)	Poisson Ratio	Density (kg/m^3)	Rupture Strain (%)
AA5010	234	215	69	0.33	2780	**7.1**
AA1100	125	41	68.9	0.33	2770	**20**

Table 4. Johnson-Cook Model Parameters [24, 25].

Material	A (Mpa)	B (Mpa)	n	m	C	T_{melt} (k)	$\dot{\varepsilon}_0$
AA5010	215	234	0.551	0.859	0.001	893	**1**
AA1100	41	125	0.183	0.859	0.001	893	**1**

1.1. Failure criterion

Structural failures under blast loading have been categorized by Menkes and Opat [26] for the first time. They carried out some tests on bars made of the Al6061-T6 alloy in 1973. Jones [27] studied this problem analytically using a rigid perfectly plastic model. These researchers categorized the failure modes into three groups. In mode I, considerable plastic deformation occurs without rupture. In mode II, the tensile rupture takes places in the vicinity of supports. In mode III, the transverse shear rupture occurs. To simulate the failure of mode II and III in the ABAQUS, the Johnson-Cook failure model was used as the damage criterion. This model is suitable for predicting damage in materials under high strain rate loadings and temperature changes. The Johnson-Cook failure model can be written as:

$$D=\sum \frac{\Delta \varepsilon_p}{\varepsilon_f} \tag{2}$$

$$\varepsilon_f=[d_1 + d_2 exp(d_3 \sigma^*)]\left[1 + d_4 ln\left(\frac{\dot{\varepsilon}_p}{\dot{\varepsilon}_0}\right)\right][1 + d_5 T^*]$$

where $\Delta\varepsilon_p$ is the increment of equivalent plastic strain, ε_f is the strain at failure, and D is the damage parameter and failure occurs when D=1. Furthermore, σ^* is the effective stress to the hydrostatic stress ratio and d_1 to d_5 are the material coefficients. In the present paper, the values of table 5 were used. To present the tearing modes, element deletion was activated to delete the damaged elements. In the next section the blast loading modeling in ABAQUS software is presented.

Table 5. Johnson-Cook Model Damage Parameters [24, 25].

Material	d_1	d_2	d_3	d_4	d_5
AA5010	0.0261	0.263	-0.349	0.147	**16.8**
AA1100	0.071	1.248	-1.142	0.0097	**0**

4. Blast loading modeling

According to the above discussion, to consider the effect of negative phase in the blast loading, the Friedlander equation was used. As this loading case due to lack of availability in the ABAQUS software, a subroutine was developed. The Friedlander equation considers the positive phase of blast wave as an exponential function as follow [28]:

$$P(t)=P_0+P_{max}\left(1+\frac{t}{t_d}\right)^{\frac{-bt}{t_d}} \qquad \text{For} \quad t < t_d \tag{3}$$

In this equation P_0, P_{max}, b, and t_d represent atmospheric pressure, peak overpressure, decay parameter, and time of duration for positive phase respectively. These parameters can be obtained as [28]:

$$\frac{P_{\max}}{P_0}=\frac{808\left[1+\left(\frac{z}{4.5}\right)^2\right]}{\sqrt{1+\left(\frac{z}{0.048}\right)^2}\sqrt{1+\left(\frac{z}{0.32}\right)^2}\sqrt{1+\left(\frac{z}{1.35}\right)^2}} \tag{4}$$

$$b= 5.2777\, Z^{-1.1975} \tag{5}$$

$$\frac{t_d}{w^{\frac{1}{3}}}=\frac{980\left[1+\left(\frac{z}{0.54}\right)^{10}\right]}{\left[1+\left(\frac{z}{0.02}\right)^3\right]\left[1+\left(\frac{z}{0.74}\right)^6\right]\left[1+\left(\frac{z}{6.9}\right)^2\right]} \tag{6}$$

$$Z=\frac{S}{W^{\frac{1}{3}}} \tag{7}$$

In Fig. 4 schematic pressure-time curve for an air blast wave and approximation of the negative phase can be seen.

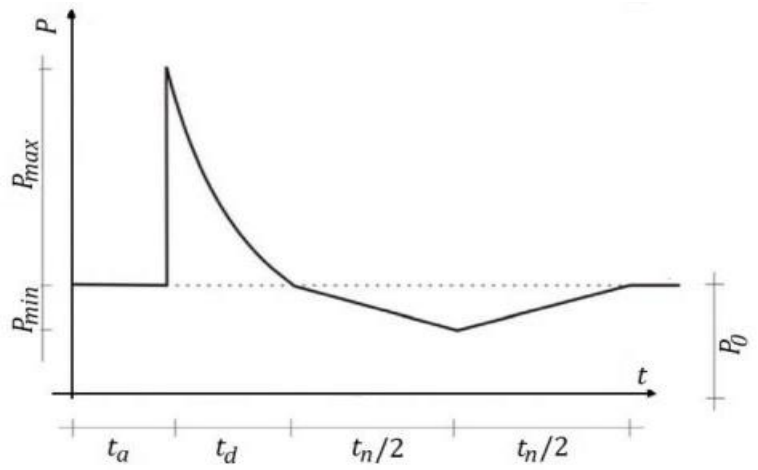

Fig. 4. Pressure-time curve for air blast wave and approximation of negative phase [21].

The effect of negative phase depends on the scaled distance. For scaled distances, as far as Z is larger than 20, the influence of negative phase cannot be neglected. It is worth to mention if a structure can withstand the positive phase successfully, it may be failed under the negative phase. The form of the negative phase is approximated by a bilinear equation as [21]:

$$P(t) = P_0 - \frac{2P_{min}}{t_n}(t - t_n) \qquad \text{For} \quad t_d + \frac{t_n}{2} < t > t_d \tag{8}$$

$$P(t) = P_0 - \frac{2P_{min}}{t_n}(t_d + t_n - t) \qquad \text{For} \quad t_d + t_n < t > t_d + \frac{t_n}{2} \tag{9}$$

In these equations P_{min} and t_n represent the maximum negative pressure and duration time of the negative phase. These parameters can be stated as [21]:

$$\begin{aligned} P_{min} &= \frac{0.35}{Z} 10^5 \text{ Pa} && \textit{For} \quad Z > 3.5 \\ P_{min} &= 10^4 \text{ Pa} && \text{For} \quad Z < 3.5 \end{aligned} \tag{10}$$

$$\begin{aligned} t_n &= 0.0104\ w^{\frac{1}{3}} && \text{For} \quad Z > 0.3 \\ t_n &= (0.003125 \log(z) + 0.01201)\ w^{\frac{1}{3}} && \text{For} \quad 1.9 \leq Z \geq 0.3 \\ t_n &= 0.0139\ w^{\frac{1}{3}} && \text{For} \quad Z > 1.9 \end{aligned} \tag{11}$$

5. Results and discussion

In this section results of simulations are described and compared with experimental data. In the first subsection, the results of the maximum deflection due to air blast are presented.

1.2. Deflection results

The results of using the conwep and Friedlander equation on specimen No.15 can be observed in Fig. 5. As it can be seen, the error between the conwep and experimental results is about 37% while the error between the Friedlander and experimental results is about 11%. In tables 6 and 7, the maximum deflection of simulations according to the Friedlander equation and maximum deflection of experimental results are given for uniform and non-uniform shock waves. As it can be seen using the Friedlander equation reduces the average error to 9.5% for non-uniform shock waves and 8% for uniform ones. Figs. 6 and 7 show the plot of deflections versus time for uniform and non-uniform shock waves using the developed Friedlander equation. Comparison between the results of tests 1 and 2 in Fig. 6 and data of table 1 reveals that the decrease of distance by 50% between the explosive mass and sheet is caused increasing of the maximum deflection by 37%. Similarly, comparison between results of tests 3 and 4 in Fig. 6 and data of table 1 predicts increase of explosive mass by 20% caused increasing of the maximum deflection by 9%.

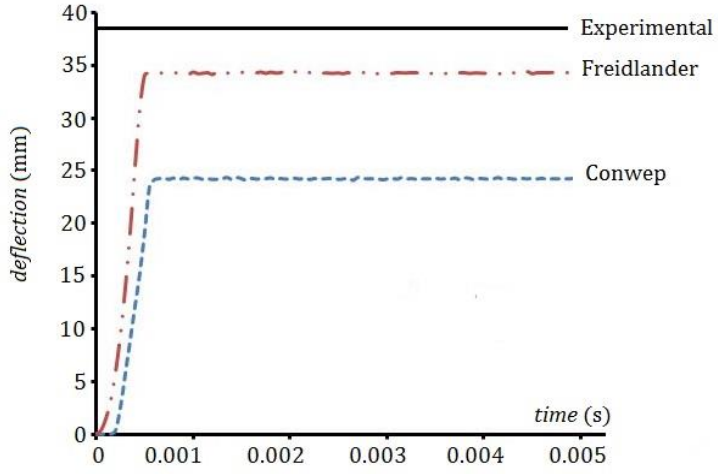

Fig. 5. Deflection-time plot for test 15.

Table 6. Simulation results in non-uniform shock wave (AA5010).

Test No.	**Deflection Experiment (mm)**	**Deflection Simulation (mm)**	**Failure Mode**	**Error**
1	12.76	14.08	I	**10.43**
2	21.40	19.32	I	**9.71**
3	32.28	19.69	I	**8.02**
4	29.84	32.30	I	**8.24**
5	-	-	II	-
6	17.18	19.11	I	**11.29**
7	32.73	29.89	I	**8.64**
8	30.24	33.01	I	**9.19**
9	31.72	35.02	I	**10.37**
10	-	-	II	-

Table 7. Simulation results in uniform shock wave (AA1100).

Test No.	Deflection Experiment (mm)	Deflection Simulation (mm)	Failure Mode	Error
11	27.75	25.4	I	8.46
12	-	-	II	-
13	29.9	27.45	I	8.19
14	31.3	33.01	I	5.46
15	38.7	34.18	I	11.67
16	-	-	II	-
17	-	-	II	-
18	23.4	21.73	I	7.13
19	28.5	26.53	I	6.91

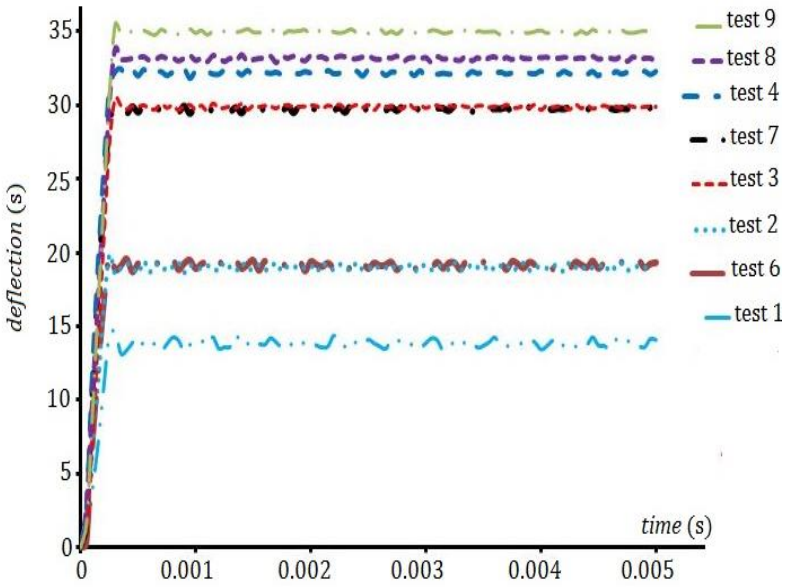

Fig. 6. Deflection-time plot in non-uniform shock wave.

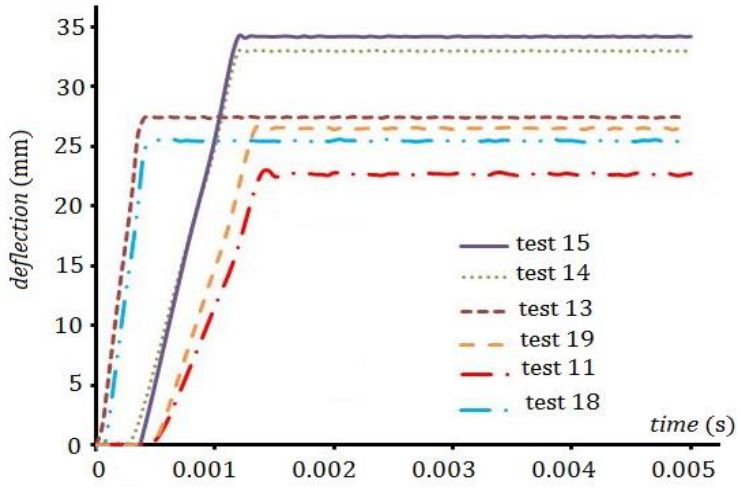

Fig. 7. Deflection-time plot in uniform shock wave.

1.3. Uniform and non-uniform shock waves range

It was found by researchers that shock waves that are interacting a plate can be uniform or non-uniform [28, 29]. In the uniform case, waves in different points are similar and the strength of shock waves is the same on the impacted plate. But, in the non-uniform case, shock waves in the center of a plate have more strength than other points and by increasing of radius from the center of plate the strength of shock waves decreases. In both cases shock waves propagate spherically but by increasing of distance from the explosive charge, the spherical waves grow and get closer to uniform state. A critical distance has been defined by researchers that for distances greater than this critical distance, the shock waves are uniform. On the other hand, for distances smaller than this critical distance the shock waves are non-uniform. In fact, the dynamic deformation response of plates is different in the uniform and non-uniform cases. In the non-uniform shock wave range, pressure in the center of plate is greater than the pressure on the edge. But, in the uniform shock wave range, pressure is the same on the center and edge of plate.

Two of tests have been designed to study the uniform pressure range. To this end, two circular plates with radius of 85 mm exposed to shock waves of 5 gr C4 explosive charge in different distances. In the ABAQUS simulations, pressure of shock waves was measured in the middle and the edge elements of plates. Results of these tests can be observed in table 8. As it can be seen from this table, increasing of distance between the center of plate and explosive charge reduces the pressure difference between the two elements. Also, at distances more than three times of the radius of plates, pressure at the center and edge elements approximately is the same as it has been concluded by other researchers [28, 29].

Table 8. Study the pressure in the edges and center plates.

Test No.	C4 (gr)	Distance to the plate (m)	Pressure in edges plates	Pressure in center plates
a	5.0	0.05	3.65	**10.1**
b	5.0	0.325	0.253	**0.271**

Figures 8 and 9 represent the pressure of center and edge of sheet over the time. As it can be seen from Fig. 8 for the case of non-uniform wave, the pressure is increased at the center during smaller time than the edge. However, as it can be observed from Fig. 9 in the case of uniform wave on plate, the wave front reaches the center and edge of plate in the same time and with equal strength.

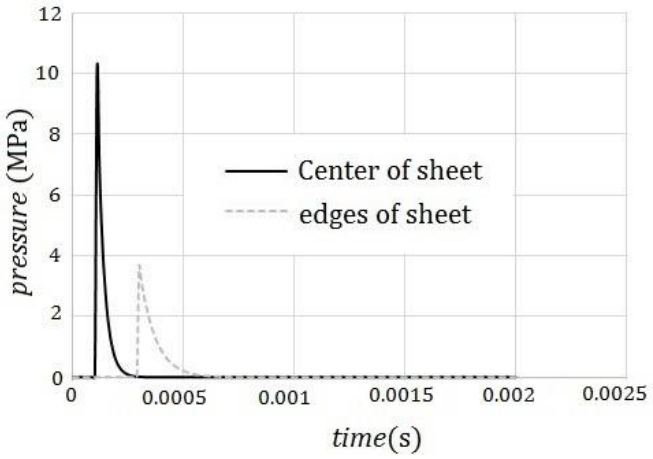

Fig. 8. Pressure-time plot at the center and edge of the sheet in test (a).

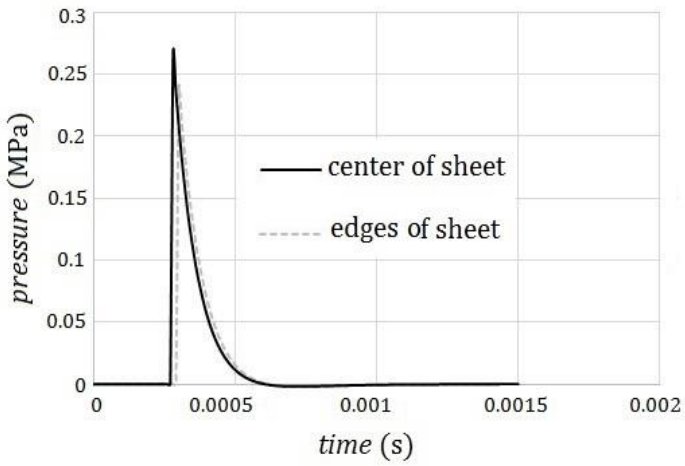

Fig. 9. Pressure-time plot at the center and edge of the sheet in test (b).

Figures 10 and 11 represent the deformed plate under non-uniform and uniform shock waves of the case (a) and (b) of table 8 respectively. As it can be seen from the contours of Fig. 11, the von-Misses equivalent stress is distributed in the narrower range with respect to Fig. 10. Also, the deformed profiles of Figs. 10 and 11 were plotted in Fig. 12. As it can be seen the non-uniform profile of the deformed shape of Fig. 10 is clear.

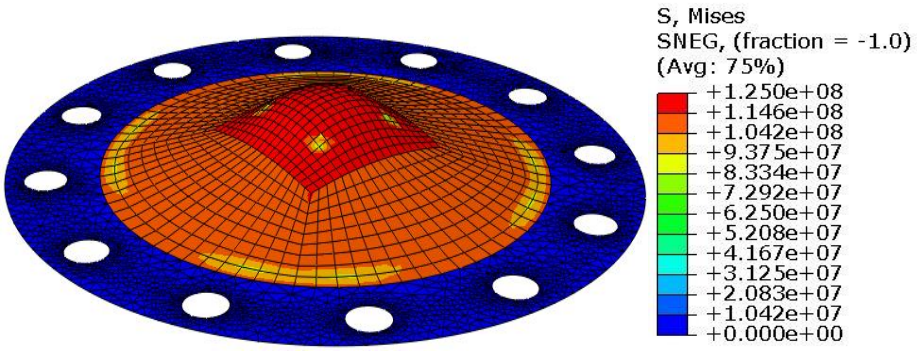

Fig. 10. von-Mises stress contours for non-uniform shock wave.

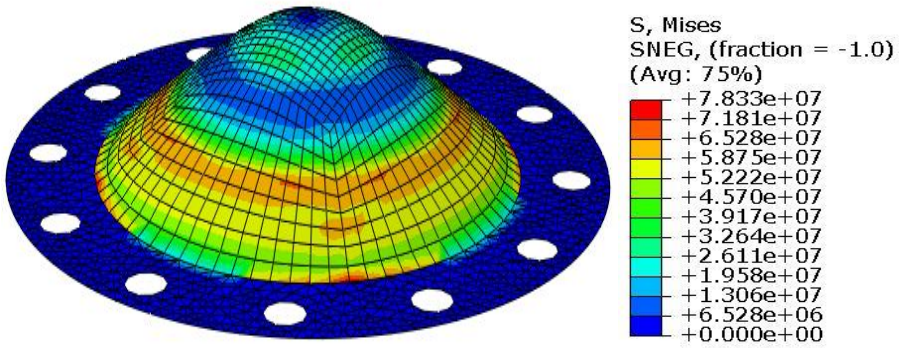

Fig. 11. von-Mises stress contours for uniform shock wave.

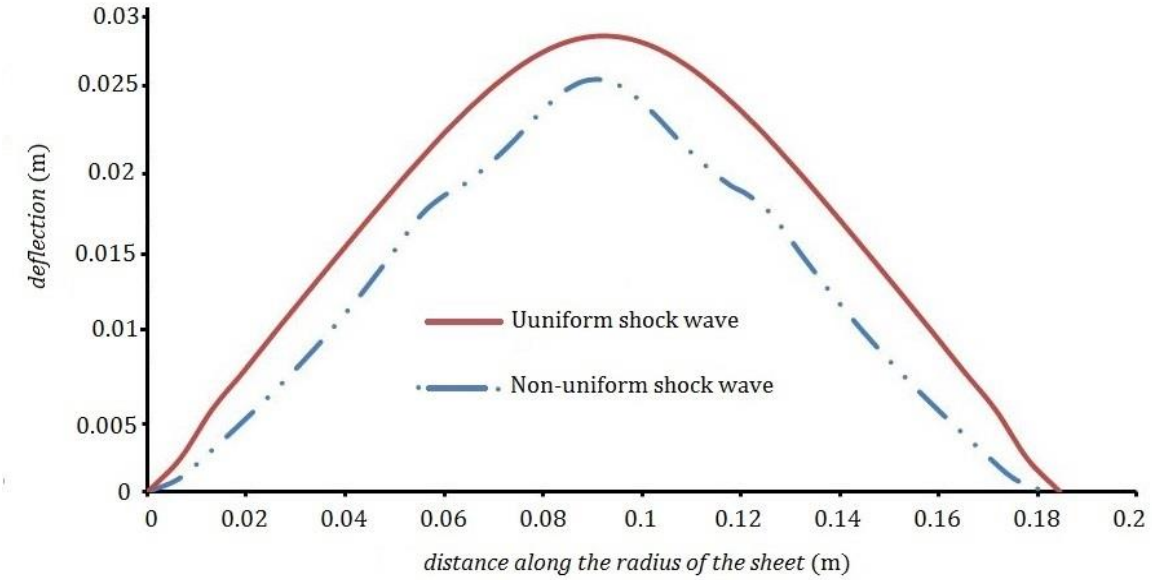

Fig. 12. Profile of uniform and non-uniform deformed shape under blast loading.

According to table 6, it can be seen about 20% of tests failed in mode II for the AA5010 alloy. Based on the information in table 7, about 33% of tests failed in this mode for the AA100 alloy. In case 17, the failure analysis was done by damage parameters mentioned in subsection 3.1 and element deletion. The results can be seen in Fig. 13 for various times of explosion. As it can be seen from the same location tearing was initiated in both of experiment and simulation. From the results of Figs. 13e and 13f, it can be concluded the onset of tearing was occurred between the 0.36 ms and 0.38 ms.

(a) (b)

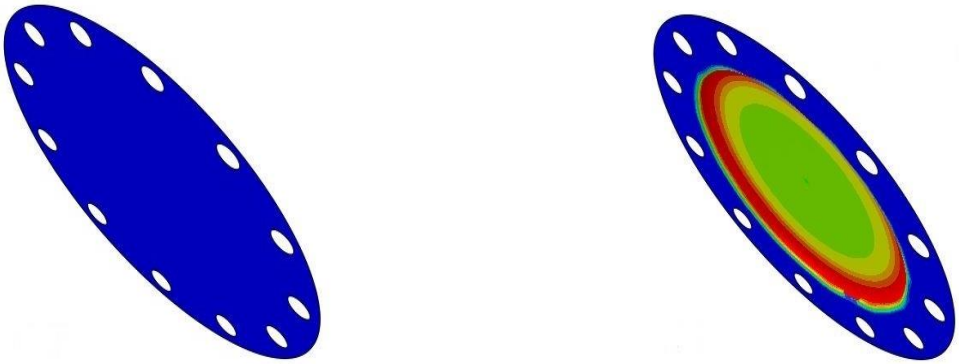

(c) (d)

(e) (f)

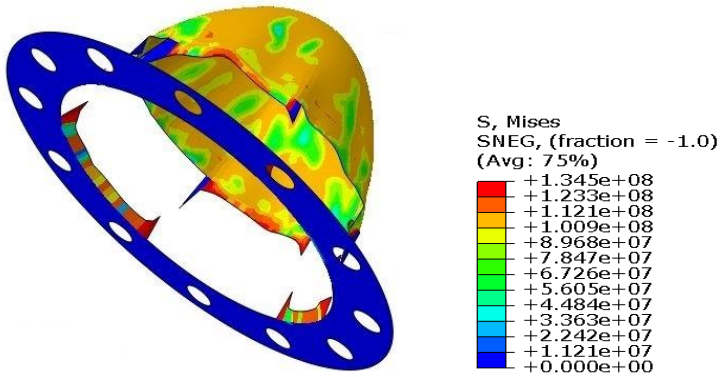

(g)

Fig. 13. Results of deformed shape on case 17: (a) tearing sheet in die set , (b) tearing sheet, and simulation results for: (c) t=0 , (d) t=0.16 ms, (e) t=0.36 ms, (f) t=0.38 ms, (g) t= 0.48 ms.

6. Conclusion

In this research, the maximum deflection of circular plates made of the AA5010 and AA1100 alloys under blast loading were studied using the ABAQUS software. Shock waves were produced by exploding of a spherical charge in different distances. In order to decrease errors due to the nature of the conwep model, a VDLOAD user subroutine was developed for the Friedlander function. Application of this subroutine reduces the error between the simulation and experimental results to 8%. Uniform and non-uniform shock waves rang and their effects on deformation and different types of failure on specimens were discussed. It was observed that at distances less than the critical one, the shock wave impacts specimens non-uniformly and thereby a non-uniform deformation occur. Because the strength of blast waves in the center was more than the edge of sheets, the risk of tearing in the center of sheets was higher than other areas. Moreover, results of damage simulation predicted the onset time of tearing.

Acknowledgments: The authors would like to thank the K. N. Toosi University of Technology, Tehran, Iran for financial support and Mr. Daemi for performing the experiments.

5. References

[1] F. W. Travis and W. Johnson, *Experiments in the dynamic deformation of clamped circular sheets of various metals subject to an underwater explosive charge*, *Sheet Met. Indust*, 39(1961) 456.

[2] W. Johnson, A. Poynton, H. Singh, and F. W. Travis, Experiments in the underwater explosive stretch forming of clamped circular blanks, *Int. J. Mech. Sci.*, 8,4(1966) 237–270.

[3] C. P. Vendhan, K. Ramajeyathilagam and V. Bhujanga Rao, Non-linear transient dynamic response of rectangular plates under shock loading, *Int. J. Impact Eng.*, 24, 10(2000) 999–1015.

[4] V. H. Balden and G. N. Nurick, Numerical simulation of the post-failure motion of steel plates subjected to blast loading, *Int. J. Impact Eng.*, 32, 1(2005) 14–34.

[5] A. Neuberger, S. Peles and D. Rittel, Scaling the response of circular plates subjected to large and close-range spherical explosions. Part I: Air-blast loading, *Int. J. Impact Eng.*, 34, 5(2007) 859–873.

[6] G. J. McShane, C. Stewart, M. T. Aronson, H. N. G. Wadley, N. A. Fleck and V. S. Deshpande, Dynamic rupture of polymer-metal bilayer plates, *Int. J. Solids Struct.*, 45, 16(2008) 4407–4426.

[7] K. Narooei and A. Karimi Taheri, A study on sheet formability by a stretch-forming process using assumed strain FEM, *J Eng Math*, (2009) 311–324.

[8] M. S. Chafi, G. Karami and M. Ziejewski, Numerical analysis of blast-induced wave propagation using FSI and ALEmulti-material formulations, *Int. J. Impact Eng.*, 36, 10(2009) 1269–1275.

[9] A. Neuberger, S. Peles and D. Rittel, Springback of circular clamped armor steel plates subjected to spherical air-blast loading, *International Journal of Impact Engineering*, (2009) 53–60.

[10] G. S. Langdon, D. Karagiozova, M. D. Theobald, G. N. Nurick, G. Lu and R. P. Merrett, Fracture of aluminium foam core sacrificial cladding subjected to air-blast loading, *Int. J. Impact Eng.*, 37, 6(2010) 638–651.

[11] J. Zamani, H. Shariati, A. Gamsari and A. Sheykhi, Effect of strain rate on the circular plate under dynamic loading by introducing a dynamic rather than static failure, *J. Energ. Mater.*, 10, 2(2011).

[12] M. D. Goel, V. A. Matsagar and A. K. Gupta, Dynamic Response of Stiffened Plates under Air Blast, *Int. J. Prot. Struct.*, 2, 1(2011) 139–156.

[13] P. Kumar, D. S. Stargel and A. Shukla, Effect of plate curvature on blast response of carbon composite panels, *Compos. Struct.*, 99(2013) 19–30.

[14] K. Spranghers, I. Vasilakos, D. Lecompte, H. Sol and J. Vantomme, Numerical simulation and experimental validation of the dynamic response of aluminum plates under free air explosions, *International Journal of Impact Engineering*, (2013) 83-95.

[15] P. Longere, A. Greza, B. Leble and A. Dragon, Ship structure steel plate failure under near-field air blast

loading: Numerical simulations vs experiment, *International Journal of Impact Engineering*, 62(2013) 88-98.

[16] H. R. Tavakoli and F. Kiakojouri, Numerical dynamic analysis of stiffened plates under blast loading, *Lat. Am. J. Solids Struct.*, 11, 2(2014) 185–199.

[17] E. Sitnikova, Z.W. Guan, G.K Schleyer and W.J. Cantwell, Modelling of perforation in fiber metal laminates subjected to high impulsive blast loading, *International Journal of Solids and Structures*, 51(2014) 3135-3145.

[18] N. Jha and B.S. Kumar, Air blast validation using ANSYS/AUTODYN, *International Journal of Engineering Research & Technology (IJERT)*, 3, 1(2014).

[19] E.A. Flores-Johnson, L. Shen, L. Guiamatsia and G.D. Nguyen, A numerical study of bioinspired nacre-like composite plates under blast loading, *Composite structures*, 126(2015) 329-336.

[20] K. Micallef, A.S. Fallah, P.T. Curtis and L.A. Louca, On the dynamic plastic response of steel membranes subjected to localised blast loading, *International Journal of Impact Engineering*, 89(2016) 25-37.

[21] M. Larcher, *Simulation of the Effects of an Air Blast Wave*, I-21020 Ispra, Italy, JRC Tech Notes, (2007) 4-17.

[22] G. F. Kinney and K. J. Graham, *Explosive shocks in air*, (1985) Second Edition 282, Berlin and New York, Springer-Verlag.

[23] T. Belytschko, W. Liu and B. Moran, *Nonlinear finite elements s for continua and structures*, (2000) Fourth Edition, 609-615,england: wiley.

[24] A. E. El Mokadem, A. S. Wifi and I. Salama, A study on the UNDEX cup forming, 37, 2(2009) pp. 556–562.

[25] G. Tiwari, M. A. Iqbal and P. K. Gupta, *Influence of Target Convexity and Concavity on the Ballistic Limit of Thin Aluminum Plate against by*, 6, 3(2013) 365–372.

[26] S. Menkes and H. Opat, Broken beams, *Eperimental Mechanics*, 13, 11(1973) pp. 480-486.

[27] N. Jones, *Structural impact*, (2011) Cambridge University Press.

[28] R. Rajendran and J. M. Lee, Blast loaded plates, *Marine Stractures*, 22(2009) 99–127.

[29] E. Borenstein and H. Benaroya, Loading and structural response model of circular plate subjected to near field explosions, *Journal of sound and Vibration*, 332(2013) 1725–1753.

بررسی عددی تغییر شکل صفحات دایروی تحت موج انفجار در هوا

بهمن ویسی، کیوان نارویی، جمال زمانی
دانشگاه صنعتی خواجه نصیرالدین طوسی، تهران، ایران

چکیده: در تحقیق حاضر ماکزیمم خیز صفحات دایروی که از آلیاژهای AA5010 و AA110 ساخته شده‌اند تحت بارگذاری انفجاری مورد بررسی قرار گرفت. موج شوک توسط انفجار خرج کروی در فواصل مختلف از مرکز صفحات دایروی تولید شد. نرم افزار آباکوس از معادله کانوب برای تحلیل بارگذاری انفجاری استفاده می‌نماید. تشخیص داده شده است که این معادله حدود 30 تا 40 درصد بی دقتی در مقایسه با نتایج آزمایشگاهی ایجاد می‌نماید. برای بهبود دقت در نتایج شبیه‌سازی از معادله فریدلندر استفاده شد که در آن فاز مثبت انفجار بصورت تابع نمایی و فاز منفی بصورت دو خطی در نظر گرفته می‌شود. در این راستا زیر برنامه VDLOAD گسترش داده شد. نتایج نشان داد که اختلاف بین نتایج آزمایشگاهی و شبیه سازی به 8 درصد کاهش یافت. همچنین تاثیر موج شوک یکنواخت و غیر یکنواخت بر روی تغییر شکل سازه و حالت‌های مختلف واماندگی بررسی شد. مشاهده شد که موج شوک یکنواخت می‌تواند زمانی حاصل شود که حداقل فاصله بین خرج انفجاری و صفحه کمتر از سه برابر شعاع صفحه باشد.

کلمات کلیدی: بارگذاری انفجاری، معادله فریدلندر، صفحه دایروی، واماندگی، شکل دادن انفجاری.